Effect of Conduit Material on CICC Performance Under High Cycling Loads

Nicolai N. Martovetsky, Pierluigi Bruzzone, Boris Stepanov, Rainer Wesche, Chen-yu Gung, Joseph V. Minervini, Makoto Takayasu, Loren F. Goodrich, Jack W. Ekin, and Arend Nijhuis

***Abstract*—Recent International Thermonuclear Experimental Reactor (ITER) Model Coils and tests on Nb_3Sn Cable in Conduit Conductors (CICC) showed a significant and unexpected increase in the broadness of the transition to the normal state, resulting in degradation of superconducting properties. To investigate these phenomena, two CICC samples were built with identical 144 strand cables but different conduit materials. One sample had titanium conduit with low coefficient of thermal expansion, the other had stainless steel conduit. The purpose of this experiment was to study changes in strand properties in the cable (critical current, current sharing temperature, n-value), the effects of cycling and high electromagnetic load, and the effect of the conduit on the CICC performance.**

***Index Terms*—Nb_3Sn cable in conduit, superconducting cables, superconducting filaments and wires.**

I. Introduction

IT IS WELL known that the Nb_3Sn critical current is sensitive to strain and therefore to the conduit material's coefficient of thermal expansion (CTE). Degradation of the superconducting properties observed in International Thermonuclear Experimental Reactor (ITER) Model Coils [1]–[4] extended our knowledge base about Nb_3Sn Cable in Conduit Conductors (CICC) and required significant conductor design changes to meet ITER requirements. Many questions about Nb_3Sn CICC behavior during high-current operation still have not been satisfactorily explained. In the Model Coils, all tested Nb_3Sn CICC performed below expectations as estimated from the mismatch between CTEs of the conduit and the strands. Especially surprising was lower than expected performance of the CICC in low-CTE conduits (Incoloy and Ti), which were expected not to degrade the superconducting cable noticeably. The Toroidal Field Model Coil (TFMC) [3], the only stainless steel (SS) CICC in this study, also showed somewhat more degradation than expected.

Model Coils also showed that cyclic loads could cause yet more degradation of properties. Degradation in critical current (I_c) can also be expressed as a decrease in the current-sharing temperature (T_{cs}). One low-CTE CICC had significant degradation (about 0.5 K) [1], and another one about 0.15 K [4]. The remaining low-CTE [2] and SS CICC [3] had cyclic degradation of less than 0.1 K, which was barely detectable.

The CICC design and analysis in ITER and many other projects are based on the correlation of Nb_3Sn performance by Summers-Ekin [5] based on intrinsic strain data above -0.4% and extrapolation to higher compressive strain when necessary. Data obtained recently by University of Durham group [6] on highly doped Nb_3Sn strands under higher uniaxial compression show a more rapid I_c drop off with strain. This difference needs to be resolved, since it is essential to have a reliable correlation for design of Nb_3Sn CICC. Such uncertainty calls for verification tests to be performed in conditions as close as possible to CICC operating conditions to limit room for errors.

The Model Coil data had limited accuracy since there was noticeable scatter in the properties of the strands used. Due to a very large magnet and difficult access, it was not always possible to place the instrumentation in the best locations. Also, it was not possible to know whether handling the conductor during fabrication after the heat treatment (HT) caused any degradation.

The objective of the experiment discussed in this paper was to study the transformation of the Nb_3Sn strand properties in CICC, based on accurate knowledge of the initial strand properties, and to compare behavior of CICC in SS and low-CTE conduits that were undisturbed by coil fabrication operations after HT. Two identical cables made from the excess IGC strand used for the Central Solenoid Model Coil (CSMC) were encapsulated into two tubes: 304 type SS and pure Ti conduits. We bent the CICC into hairpin samples and heat-treated them. We instrumented the samples with voltage taps and temperature sensors, and tested the samples in fields up to 11 T in SULTAN facility at CRPP, Switzerland. To eliminate the current redistribution problems, the cable terminations were stripped of Cr plating and filled with SnAg solder. The conductors' layout is given in Table I.

Manuscript received October 5, 2004. This work was supported by the U.S. Department of Energy under contract to the Lawrence Livermore National Laboratory (Contract W-7405-Eng-48), the Massachusetts Institute of Technology under Grant DE-FC02-93ER54186-D&T, and by the European Fusion Technology Program. The contribution of NIST is not subject to copyright. Certain commercial materials are referred to in this paper to foster understanding. Such identification does not imply recommendation or endorsement by NIST, nor does it imply that the materials identified are necessarily the best available for the purpose.

N. N. Martovetsky is with Lawrence Livermore National Laboratory, Livermore, CA 94550 USA (e-mail: martovetsky1@llnl.gov).

P. Bruzzone, B. Stepanov, and R. Wesche are with the Centre de Recherches en Physique des Plasmas (CRPP), CH-5232 Villigen-PSI, Switzerland (e-mail: pierluigi.bruzzone@psi.ch).

C. Gung, J. V. Minervini, and M. Takayasu are with Plasma Science and Fusion Center, Massachusetts Institute of Technology, Cambridge, MA 02139 USA (e-mail: minervini@psfc.mit.edu).

L. F. Goodrich and J. W. Ekin are with the National Institute of Standards and Technology (NIST), Boulder, CO 80305 USA (e-mail: goodrich@boulder.nist.gov).

A. Nijhuis is with University of Twente, 7500 AE Enschede, The Netherlands (e-mail: a.nijhuis@tn.utwente.nl).

Digital Object Identifier 10.1109/TASC.2005.849091

TABLE I
TESTED CICC PARAMETERS

	SS	TI
Nb_3Sn strand diameter, mm	0.81	
Cu:non-Cu	1.5 ± 0.05	
Cr plating thickness, μm	2	
Cable configuration	3 x 3 x 4 x 4 = 144	
Cable pitches, mm	10 / 51 / 79 / 136 / 166 right hand	
Void fraction, %	≈ 33.1	
CICC diameter, mm	14.51 – 14.57	14.56 – 14.59
Jacket material	Stainless steel 12X18H110T	Ti (grade 2)

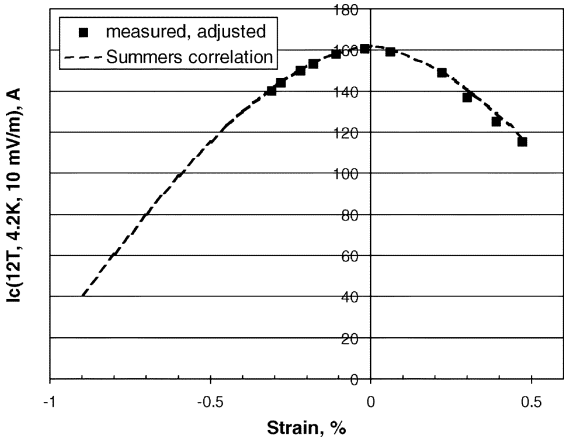

Fig. 1. Strain sensitivity of the IGC strand at 12 T and 4.2 K.

II. STRAND CHARACTERIZATION

The strand properties were measured in several laboratories: NIST, MIT, CRPP and UT. UT measured strain effect at two temperatures(work is still in progress), NIST and CRPP performed measurements at variable temperatures, while all MIT data were taken at 4.2 K. The scatter among the NIST, UT, and CRPP data without applied strain was small; MIT data were 2 to 3% lower. The strand properties without applied strain can be satisfactorily described by the Summers (also known as the Summers-Ekin) correlation [5] with the following parameters: $C_0 = 11\,776\,\mathrm{A}\cdot\mathrm{T/mm}^2$, $T_{\mathrm{c0m}} = 16.8\,\mathrm{K}$, $B_{\mathrm{c2m}} = 28.5\,\mathrm{T}$, assuming resulting stress of -0.25%. The strain sensitivity was measured at NIST on an identical strand that had undergone a slightly different heat treatment, resulting in 11% higher I_{c} (12 T, 4.2 K, 10 $\mu\mathrm{V/m}$). These data, after an 11% reduction in I_{c}, are shown in Fig. 1 along with the Summers correlation.

III. CICC WITH SS CONDUIT

The test procedure for the samples was as follows. After calibration runs and checks and AC tests with no transport current, T_{c0m} measurements were attempted but were not very successful due to hydraulic instabilities above 15 K. I_{c} was then measured in the background field. We started at the lowest $I\times B$ force at 11 T and 8 K to find out whether the first cycle of electromagnetic loading is important in the degradation evolution. I_{c} and T_{cs} were measured at 10 $\mu\mathrm{V/m}$ over 30 cm in the high-field region. I_{c} was measured by sweeping the current at constant temperature. T_{cs} was measured by sweeping the temperature at constant current. All data were taken at a He flow rate of 3 g/s through each leg. Test results on the SS sample before cycling are shown in Fig. 2. The arrows for 11 T measurements indicate the sequence of I_{c} measurements. We see that after the CICC was exposed to the highest $I\times B$, I_{c} noticeably decreased, which shows that the very first loading affects the strand properties.

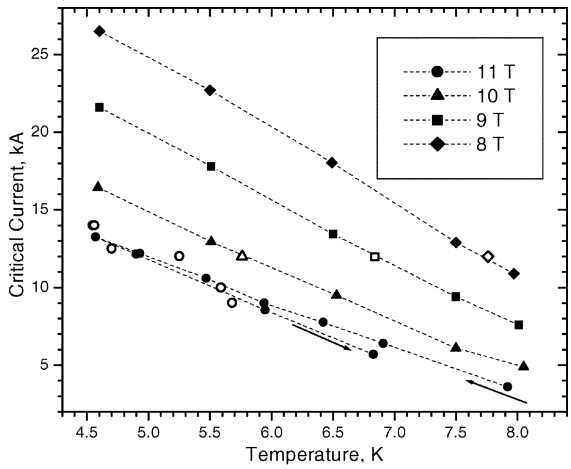

Fig. 2. I_{c} (solid) and T_{cs} (open symbols) of SS CICC before cycling.

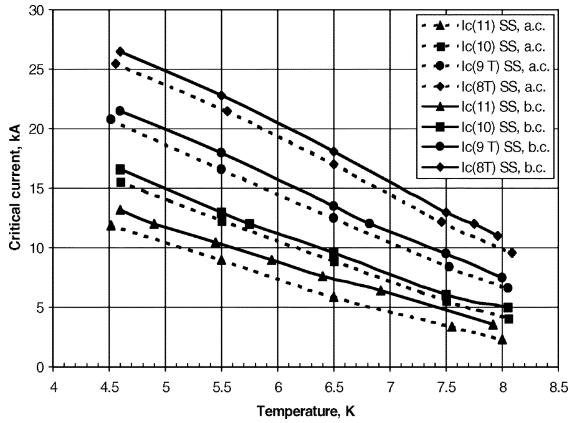

Fig. 3. I_{c} (10 $\mu\mathrm{V/m}$) in the SS CICC before and after cycles.

After cycling from 0 to 17 kA at 10 T and 4.5 K, the properties of the CICC degraded in a more continuous manner. I_{c} of the SS sample came to saturation after about 600 cycles, as shown in Fig. 3. The nomenclature "b.c." corresponds to "before cycles" and "a.c." to "after cycles". The I_{c} dropped by 10 to 20% (higher in higher field) and in terms of T_{cs}, by about 0.5 K at 11 T. This agrees with data for the ITER CS Insert, which saturated at a similar number of cycles. Similar to this work, samples measured at SULTAN in 2001 [7] had I_{c} saturated after about 2500 cycles, but the I_{c} degradation was about 20%.

IV. CICC WITH Ti CONDUIT

The CICC with Ti conduit tests were conducted in the same manner as the CICC with SS conduit. The Ti conduit sample had higher initial I_{c} and quench current (I_{q}, current at thermal runaway), as expected. The degradation of current as a result of cycling was similar to the SS CICC.

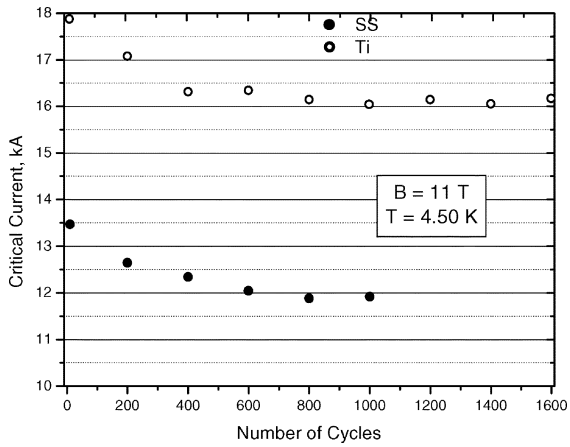

Fig. 4. Evolution of I_c as a result of load cycles.

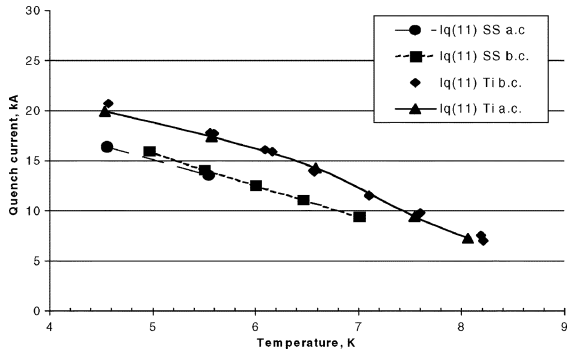

Fig. 5. Quench current in CICC at 11 T before and after the cycles. The lines are to guide the eye.

Fig. 4 shows the comparative degradation of the CICCs studied. The ratio between I_c (Ti) and I_c (SS) versus cycles at 11 T and 4.5 K always was in the range of 1.32 to 1.36.

In agreement with earlier results reported in [7], the I_q changed much less than I_c due to cycles. Fig. 5 compares I_q for both CICCs. I_q depends on the helium mass flow and length of the conductor in the peak field [8]; therefore its value depends not only on the superconducting properties, such as I_c, but also on operating conditions. Both I_c and I_q of the low-CTE Ti conduit show about a 30% advantage over the SS conduit at 11 T and 4.5 K. At 12 kA and 11 T, the Ti CICC has a T_{cs} about 1.3 K higher than the SS CICC. This result is consistent with the ITER Model Coil results [4], where similar performance strands (Furukawa and Europa Metalli) had about a 25 to 30% advantage in Incoloy 908 conduit (CS Insert) versus SS conduit and structure (TFMC). This advantage is lower than the 50 to 60% expected, based on the Summers correlation. Such a small difference in I_q, with a noticeable reduction of I_c as a result of the cyclic loads, can be explained by a reduction of the n-value of the resistive transition, expressed as $E = (10^{-5}) * (I/I_c)^n$ [V/m], where I_c is defined at the level of 10^{-5} V/m. Fig. 6 summarizes the n-value for the original strands and for both CICCs. As in the ITER Model Coils, the n-value for CICC is significantly lower than that in the stand-alone strand, including the data before loading and at minimal $I \times B$ values. This suggests that the degradation

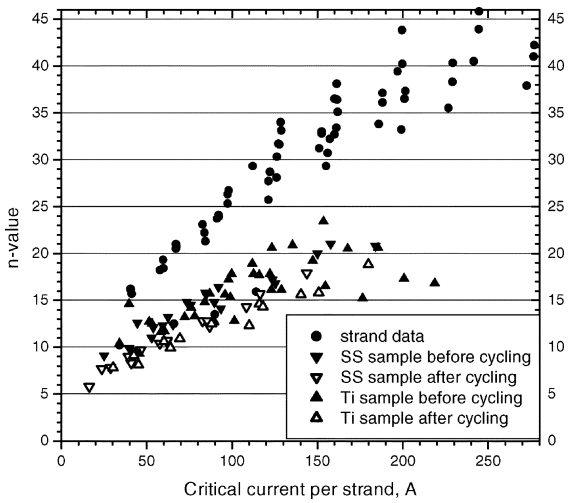

Fig. 6. Summary of the n-value measurements.

in the strands is at least partially caused by heat treatment in a conduit and subsequent cool-down. Quantitatively, the n-value for low CTE conduits tested at Model Coils (about 8 at 40 A per strand) [1] is similar to values observed in our tests, whereas the n-value measured in the TFMC (about 7–9 at 111 A per strand) is significantly lower than for SS CICC. It is unexpected to see that the low-CTE conduit did not produce higher n-values in the cable than in the SS conduit. Strand data [6], [9] on I_c versus strain always showed a higher I_c associated with a higher n-value.

V. Post-Test Analysis and Discussion

We assume that the current is uniformly distributed over the cable, which is confirmed by negligible voltage measured across the cross section. Thus, the CICC transition represents purely strand behavior, not current transfer between the strands. To compare performance of the strand with the CICC, we need to account for where the cabled strand is located in CICC in a variable field due to the transport current self-field. We used a double spiral to model the four-stage cable, modeling only the two most important last cabling stages, and calculated the electrical field along the length of the strand. The integrated electrical field should be compared to the measured electrical field. For the sake of analysis, the varying magnetic field along the length of the strand between the voltage taps is replaced with a single value of the "effective magnetic field," which is found to fit the integrated electrical field along the strand. This effective magnetic field, B_{eff}, depends on the n-value. For an n-value of 10, B_{eff} is approximately equal to the median magnetic field between the peak and average in the cable cross section. That is, $B_{eff} = (B_{peak} + B_{average})/2 = B_{sultan} + kI$, where coefficient k is computed to be 0.02 T/kA and I is the transport current. At the highest transport currents of 30 kA, the effective magnetic self-field is calculated to be 0.6 T and the peak electrical field is about four times higher than the measured average electrical field.

The anticipated strain of the Nb_3Sn strands in the SS conduits, after cool-down, is between -0.55% to -0.75%. For the Ti CICC we anticipated about -0.2% to -0.3%.

TABLE II
FITTING PARAMETERS FOR THE STRAIN IN CICC

	$\varepsilon_{cd}[\%]$	a [1/κA∗T]
Ti CICC b.c.	-0.458	-4.20e-6
Ti CICC a.c.	-0.539	-2.65e-6
SS CICC b.c	-0.600	-6.91e-6
SS CICC a.c.	-0.683	-3.75e-6
Ti TF Insert in SS structure [11]	-0.575	-2.58e-6
SS TFMC [3,10]	-0.66	-2.3e-6
Incoloy CS Insert [10] b.c.	-0.32	-3.5e-6
Incoloy CS Insert b.c. [12]	-0.45	n/a
Incoloy CS Insert a.c. [12]	-0.56	n/a

Although the Summers correlation may not be accurate for high compressive strains, we assess the CICC performance using the correlation in the full range of the strain, since we do not have reliable data and correlation for high compressive strain yet. This approach may mean that the strain deduced from the test data may be merely a fitting parameter rather than a real strain in the strands. But even such reservation makes analysis valuable for comparison with the Model Coils results. Also, the model can be used for CICC design if the operating conditions are not far from the test conditions.

In the Model Coil analysis, the Summers correlation was used to compare the performance of the strand in the CICC and of a stand-alone strand. It was found [3], [10] that this correlation can describe the parameters of the CICC if a fitting parameter is introduced in the form of an extra strain $(\varepsilon_{\mathrm{extra}})$ in addition to cool-down $(\varepsilon_{\mathrm{cd}})$ and operating-hoop strain (ε_{op}, zero in our test): $\varepsilon = \varepsilon_{cd} + \varepsilon_{op} + \varepsilon_{\mathrm{extra}}$. This additional strain is assumed to be $\varepsilon_{\mathrm{extra}} = aIB$, which takes into account the transverse force crushing and bending the strands in the cable in the lateral direction; this is just a common-sense speculation. Using this approach we found the best fit to describe the test data and results using the Summers correlation.

The fitting results are given in Table II in terms of cool-down strain and coefficient for the extra strain. Analysis data from the Model Coil program are shown for comparison and indicate that a low-CTE conduit gives a much better Nb_3Sn CICC performance compared with the SS. The advantage, however, is less than expected from I_{c} versus uniaxial strain data.

VI. CONCLUSION

Low-CTE conduit maintains its significant advantage in I_{c} and I_{q} over the SS conduit in all tested conditions. Both CICC's experience about 10% degradation in I_{c} due to cycling, suggesting that the effect of cycling on I_{c} is insensitive to the conduit material.

Even with careful handling after heat treatment, the degradation in I_{c} for the CICC with low CTE is comparable to the degradation seen in CSMC, CS and TF inserts. We see degradation even before high electromagnetic loads are applied. Thus, low-CTE conduits do not completely eliminate I_{c} degradation and is suggests that the CICCs in the Model Coil program were not damaged during fabrication.

The n-value in the low-CTE conduit CICC is only slightly higher than that in the SS conduit; both are a little more than one half that of the original strand, which is unexpected and yet to be explained.

The subscale tests reproduced many Model Coil program results and gave valuable data for a CICC design database.

ACKNOWLEDGMENT

The authors are grateful to V. E. Sytnikov and the VNIIKP group for fabrication of the CICCs, and to the CRPP personnel for preparing and running the test.

REFERENCES

[1] N. Martovetsky, P. Michael, and J. Minervini *et al.*, "ITER CS model coil and CS insert test results," *IEEE Trans. Appl. Supercond.*, vol. 11, no. 1, pp. 2030–2033, Mar. 2001.

[2] N. Martovetsky and M. Takayasu *et al.*, "Test of the ITER TF insert and central solenoid model coil," *IEEE Trans. Appl. Supercond.*, vol. 13, no. 2, pp. 1441–1446, Jun. 2003.

[3] R. Zanino, M. Bagnasco, and G. Dittrich *et al.*, "T_{cs} tests and performance assessment of the ITER toroidal field model coil (Phase II)," *IEEE Trans. Appl. Supercond.*, vol. 14, no. 2, pp. 1519–1522, Jun. 2004.

[4] K. Okuno, N. Martovetsky, and N. Koizumi *et al.*, "Test of the NbAl insert and ITER central solenoid model coil," *IEEE Trans. Appl. Supercond.*, vol. 13, no. 2, pp. 1437–1440, Jun. 2003.

[5] L. T. Summers and M. Guinan *et al.*, "A model for the prediction of Nb3Sn critical current as a function of field, temperature and radiation damage," *IEEE Trans. Magn.*, vol. 27, no. 2, pp. 2041–2044, Mar. 1991.

[6] S. A. Keyes and D. P. Hampshire, "A scaling law for the critical current density of weakly- and strongly-coupled superconductors, used to parameterize data from a technological Nb_3Sn strand," *Supercond. Sci. Tech.*, vol. 16, pp. 1097–1108, 2003.

[7] P. Bruzzone, A. Fuchs, B. Stepanov, and G. Vecsey, "Performance evolution of Nb_3Sn cable-in-conduit conductors under cyclic load," *IEEE Trans. Appl. Supercond.*, vol. 12, no. 1, pp. 516–519, Mar. 2002.

[8] N. Martovetsky, "Stability and thermal equilibrium in cable-in-conduit conductors," *Physica C: Supercond.*, vol. 401, pp. 118–123, 2004.

[9] A. Godeke, H. G. Knoopers, A. Nijhuis, H. J. G. Krooshoop, B. ten Haken, and H. H. J. ten Kate, "Characterization of ITER Strands in the Frame of the Third Benchmark Tests,", Report UT-NET 98-5, Apr. 1998.

[10] N. Mitchell, "Summary, assessment and implications of the ITER model coils test results," *Fusion Engineering and Design*, vol. 66–68, pp. 971–993, 2003.

[11] D. Bessette, "Modeling techniques for correcting measured data on the ITER toroidal field insert coil," *IEEE Trans. Appl. Supercond.*, vol. 14, no. 2, pp. 1418–1422, Jun. 2004.

[12] N. Martovetsky, "T_{cs} and I_{c} measurements in CSMC," presented at the JAERI Meeting on CSMC Test Results, Naka, Japan, Nov. 2000.